Synthesis and Crystal Structure of an Oxovanadium(IV) Complex with a Pyrazolone Ligand and Its Use as a Heterogeneous Catalyst for the Oxidation of Styrene under Mild Conditions

Sanjay Parihar,[†] Soyeb Pathan,[†] R. N. Jadeja,*,[†] Anjali Patel,*,[†] and Vivek K. Gupta[‡]

[†]Department of Chemistry, Faculty of Science, The Maharaja Sayajirao University of Baroda, Vadodara 390 002, India
[‡]Post-Graduate Department of Physics, Jammu University, Jammutawi 180 006, India

Ⓢ Supporting Information

ABSTRACT: 1-Phenyl-3-methyl-4-touloyl-5-pyrazolone (ligand) was synthesized and used to prepare an oxovanadium-(IV) complex. The complex was characterized by single-crystal X-ray analysis and various spectroscopic techniques. The single-crystal X-ray analysis of the complex shows that the ligands are coordinated in a syn configuration to each other and create a distorted octahedral environment around the metal ion. A heterogeneous catalyst comprising an oxovanadium(IV) complex and hydrous zirconia was synthesized, characterized by various physicochemical techniques, and successfully used for the solvent-free oxidation of styrene. The influence of the reaction parameters (percent loading, molar ratio of the substrate to H_2O_2, amount of catalyst, and reaction time) was studied. The catalyst was reused three times without any significant loss in the catalytic activity.
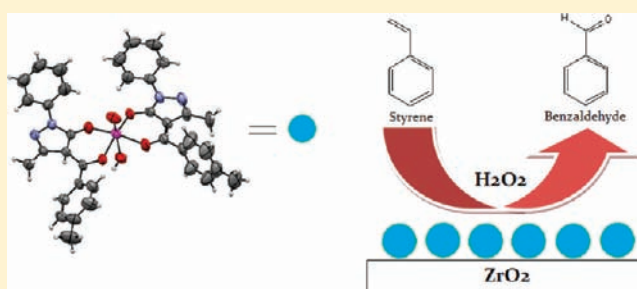
INTRODUCTION

The coordination chemistry of vanadium, in particular with multidentate ligands, is receiving much attention because of its involvement in various biological processes: in the active site of metalloenzymes such as vanadium nitrogenase[1] and haloperoxidases,[2] as a metabolic regulator,[3] as a mitogenic activator, and especially as an insulin-mimicking agent.[4] Vanadium complexes can also affect the cardiac abnormality associated with diabetes mellitus[5] and exhibit anticancer activity.[6]

Moreover, catalytic applications have also stimulated the coordination chemistry of vanadium, and the search for novel vanadium complexes with pharmacological and catalytic significance is a matter of a high current interest. Oxovanadium peroxo complexes efficiently oxygenate organic compounds. Vanadium complexes possess versatile oxidation states and unusual redox ability. Usually, vanadium can exist in 3+, 4+, and 5+ oxidation states. In 4+ and 5+ oxidation states, vanadium has strong redox ability, which can lead to some important reactions.[7] Oxovanadium complexes were illustrated to be catalysts[8] in a variety of asymmetric reactions such as the cyanation reaction,[9] epoxidation of allyl alcohols,[8a,10] oxidative coupling of 2-naphthol,[11] oxidation of organic sulfides,[8a,12] alkynyl addition to aldehydes,[13] and others.[14]

Immobilization of metal complexes onto the surfaces of solid supports is highly desirable in the development of reusable catalysts.[15] Supported vanadium oxide catalysts constitute a very important class of catalytic materials. They have become the model for catalytic systems for fundamental studies of supported metal oxides, and they are widely used as selective

oxidation catalysts in the industrial production of economically attractive redox reactions. These heterogeneous catalysts, mostly deposited on a porous support, have the advantage of mechanical strength and easy recovery and recycling, in comparison with their analogous homogeneous counterparts.

Catalytic oxidation of alkenes into more valuable epoxides as well as oxygen-containing carbonyl compounds is one of the important synthetic reactions. Carbonyl compounds have industrial significance and are widely used as solvents, perfumes, and flavoring agents or as intermediates in the manufacture of plastics, dyes, and pharmaceuticals.

As per our knowledge, only one report on the use of an oxovanadium complex with a pyrazolone ligand as a homogeneous catalyst is available.[16] Recently, the synthesis, characterization, and liquid-phase oxidation of styrene by a series of supported benzimidazole-based oxovanadium complexes have been reported by Maurya et al.[17] Thus, a literature survey shows that no reports on the catalytic aspects of supported oxovanadium complexes with pyrazolone ligands are available. In this article, we report the synthesis and characterization of an oxovanadium complex (VOL_2). The synthesized complex was heterogenized by supporting onto hydrous zirconia (ZrO_2). There are two reasons for selecting ZrO_2 as the support: (1) the available surface hydroxyl groups of ZrO_2 are able to undergo a chemical reaction or strong

Scheme 1. Synthetic Route for the Ligand L
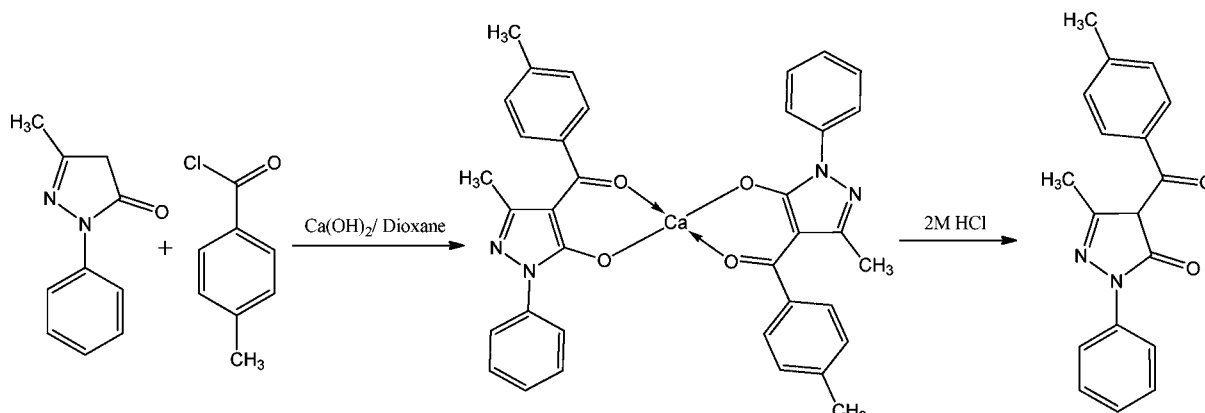
Scheme 2. General Procedure for the Synthesis of VOL$_2$
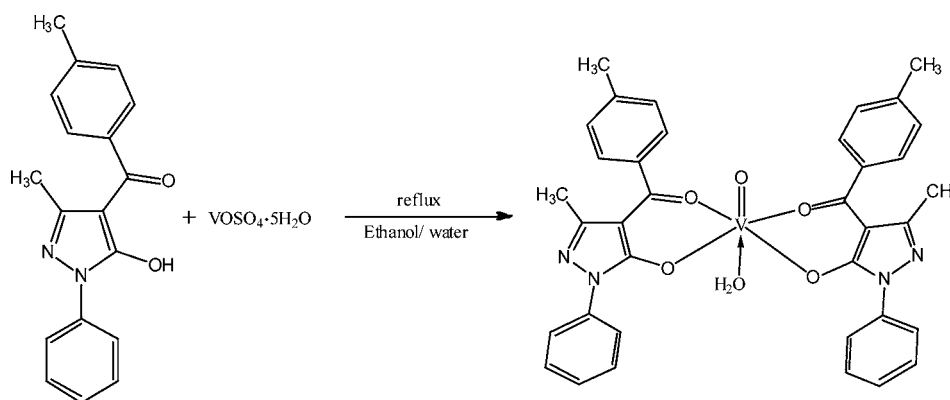
interaction with supported species[18] and (2) our expertise in using hydrous zirconia as the support.[19]

Supported complex VOL$_2$/ZrO$_2$ was characterized by various physicochemical techniques, and its catalytic activity was evaluated for the solvent-free oxidation of styrene with H$_2$O$_2$ as an oxidant under mild reaction conditions. The conditions for maximum conversion as well as selectivity for the desired product were optimized by varying different parameters such as the percent loading, molar ratio of substrate to H$_2$O$_2$, amount of the catalyst, and reaction time. The catalytic property for a recycled catalyst was also evaluated for the oxidation of styrene under optimized conditions. A reaction mechanism for the oxidation of styrene with H$_2$O$_2$ as an oxidant was proposed. A schematic representation of the ligand L is shown in Scheme 1.

■ EXPERIMENTAL SECTION

Materials. All reagents and solvents were purchased from commercial sources and were further purified by standard methods, if necessary. 1-Phenyl-3-methyl-5-pyrazolone was obtained from Nutan Dye Chem. Sachin, Surat, India. Zirconium oxychloride (Loba chemie, Mumbai, India), oxovanadium sulfate, dichloromethane, 30% aqueous H$_2$O$_2$, and styrene were obtained from Merck and used as received.

Characterization Techniques. The synthesized materials were characterized by ^{1}H NMR, gas chromatography—mass spectrometry (GC—MS), single-crystal X-ray diffraction (XRD), thermogravimetric analysis (TGA), Fourier transform infrared (FT-IR), electron spin resonance (ESR), Brunauer—Emmett—Teller (BET) surface area, and scanning electron microscopy (SEM). ^{1}H NMR spectra of the ligand L were recorded with a AV 400 MHz Bruker FT-NMR instrument. Mass spectra of the ligand L were recorded on a Trace GC ultra DSQ II.

Elemental analyses of C, H, and N were determined using a Perkin-Elmer series-II 2400 elemental analyzer. X-ray intensity data of 34 372 reflections (of which 5527 unique) were collected on a Bruker CCD area-detector diffractometer equipped with graphite-monochromated Mo Kα radiation (λ = 0.710 73 Å). A simultaneous TGA—differential thermal analysis (DTA) of VOL$_2$ and 30% VOL$_2$/ZrO$_2$ was carried out on a SII EXSTAR6000 TG/DTA 6300. The experiments were performed in N$_2$ at a heating rate of 10 °C min^{-1} in the temperature range 25−500 °C using an aluminum pan. FT-IR spectra of VOL$_2$ and 30% VOL$_2$/ZrO$_2$ were recorded as KBr pellets on a Perkin-Elmer FT-IR spectrum RX 1 spectrometer. ESR spectra of VOL$_2$ and 30% VOL$_2$/ZrO$_2$ were recorded on an X-band instrument at ESR Laboratory, SAIF, IIT, Bombay, India, at room and liquid-nitrogen temperature. Electrospray ionization mass spectrometry (ESI-MS) spectra were recorded on a Waters Q-ToF micromass. The BET specific surface areas of VOL$_2$ and 30% VOL$_2$/ZrO$_2$ were calculated using the standard BET method on the basis of the adsorption data. Metal contents were measured by inductively coupled plasma atomic emission spectroscopy (ICP-AES; Perking-Elmer Pptima 2000). Adsorption—desorption isotherms of the samples were recorded on a Micromeritics ASAP 2010 surface area analyzer at −196 °C. SEM analyses of ZrO$_2$, VOL$_2$, and 30% VOL$_2$/ZrO$_2$ were carried out using a JSM 5610 LV combined with an INCA instrument for energy-dispersive X-ray (EDX)—SEM.

Catalytic Reaction. The oxidation reaction was carried out in a borosilicate glass reactor provided with a double-walled condenser containing catalyst, styrene, and H$_2$O$_2$ at 80 °C with constant stirring for 24 h. Similar reactions were carried out by varying different parameters such as the percent loading, molar ratio of substrate to H$_2$O$_2$, amount of the catalyst, and reaction time. After completion of the reaction, catalyst was removed and the product was extracted with dichloromethane. The product was dried with magnesium sulfate and analyzed on a gas chromatograph using a BP-5 capillary column. The

Table 1. Crystal Data and Structure Refinement Details for VOL$_2$·H$_2$O

empirical formula	C$_{36}$H$_{34}$N$_4$O$_6$V
M_w (g mol^{-1})	669.61
cryst color, size (mm^3)	blue, 0.3 × 0.2 × 0.1
cryst syst	monoclinic
unit cell dimens	a = 13.6618(12) Å, b = 27.5554(17) Å, c = 9.7253(10) Å, β = 104.747(10)°
unit cell volume	3540.6(5) Å^3
space group	$P2_1/c$
no. of molecules per unit cell, Z	4
reflns collected/unique	34 372/5527
R_{int}	0.1278
R_σ	0.1027
θ range for the entire data collection (deg)	3.34 < θ < 24.00
range of indices	h = −15 to +15, k = −31 to +31, l = −11 to +11
final R	0.0768
wavelength (Å)	0.710 73
density (calcd) (Mg m^{-3})	1.256
refinement	full-matrix least squares on F^2
$R_w(F^2)$	0.1795
no. of param refined	432
GOF	0.993
final residual electron density (e Å^{-3})	−0.370 < $\Delta\rho$ < 0.374
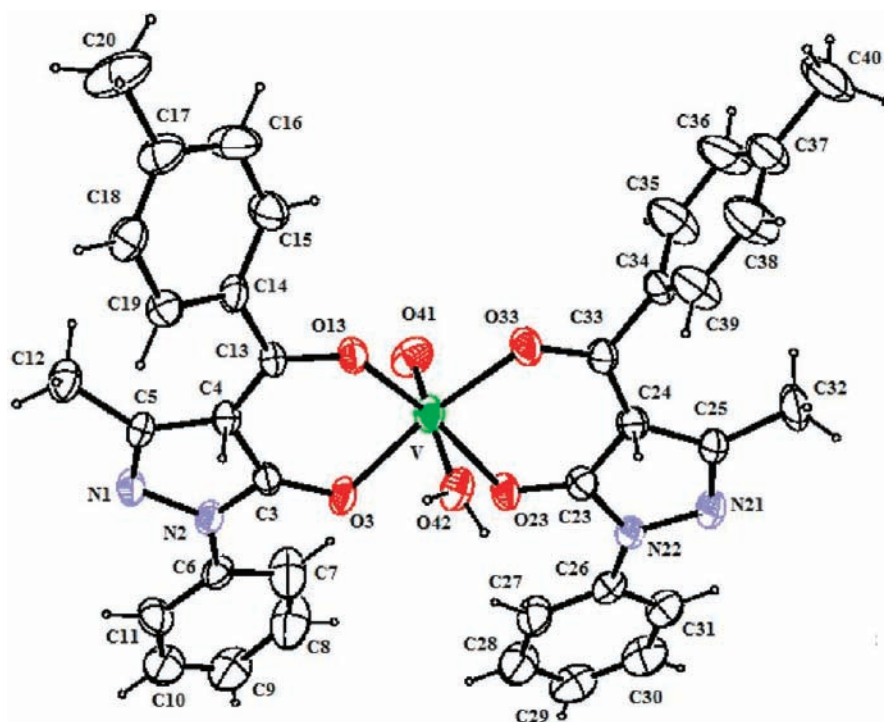
Figure 1. ORTEP view of VOL$_2$·H$_2$O with displacement ellipsoids drawn at 50%.

product was identified by comparison with the authentic samples and finally by GC−MS.

Synthesis of Ligand L. The ligand was synthesized according to the method reported previously.[20] 1-Phenyl-3-methyl-5-pyrazolone (17.4 g, 0.1 mol) and 80 mL of 1,4-dioxane were placed in a three-necked 250 mL flask equipped with a stirrer, an addition funnel, and a reflux condenser. The reaction mass was heated at 70 °C for 10 min. To the resulting yellow solution was added in small portions calcium hydroxide (14.82 g, 0.2 mol), and then the corresponding acyl chloride (15.5 g, 0.1 mol) was added dropwise. During this addition, the whole mass was converted into a thick paste. After the complete addition, the reaction mixture was heated to reflux for 2 h. The yellowish mixture was cooled to room temperature and poured into a 250 mL solution of ice-cold hydrochloric acid (2 mol L^{-1}) under stirring. The yellow

precipitate was filtered, washed with water, and dried in a vacuum. After drying, a pale-yellow solid was obtained and recrystallized from an acidified methanol−water mixture (22.79 g, 78%). Mp: 120 °C. ^{1}H NMR (400 MHz, CDCl$_3$, TMS): δ 2.47 (s, 3H), 2.16 (s, 3H), 7.88−7.9 (d, 2H), 7.57−7.59 (d, 2H), 7.46−7.5 (t, 2H), 7.3−7.34 (t, 3H). ^{13}C NMR (CDCl$_3$): δ 191.6, 161.77, 147.93, 142.72, 137.28, 134.63, 129.14, 129.1, 128.21, 126.62, 120.72, 103.56, 21.70, 16.04. Elem anal. Calcd for C$_{18}$H$_{16}$N$_2$O$_2$: C, 73.95; H, 5.52; N, 9.58. Found: C, 74.24, H, 5.58; N, 9.57. EI-MS: m/z 292.07 (calcd: m/z 292.33).

Synthesis of an Oxovanadium(IV) Complex (VOL$_2$). To a well-stirred hot ethanolic solution of ligand L (0.292 g, 0.01 mol) was added dropwise an aqueous solution of VOSO$_4$·5H$_2$O (0.127 g, 0.005 mol). The reaction mixture was refluxed for 6 h. A pale-green precipitate were formed, which was filtered, washed with hot distilled

water and then ethanol, and dried under a vacuum (see Scheme 2). The solid product was dissolved in hot MeCN and allowed to crystallize at room temperature. Blue crystals of single-crystal XRD quality were obtained in 2–4 days. The obtained material was designated as VOL_2. Yield: 0.210 g (72%). Elem anal. Calcd for $C_{36}H_{32}N_4O_6V$: C, 64.77; H, 4.83; N, 8.39. Found: C, 64.71; H, 4.87; N, 8.40. MS: m/z 650.14 $([M + H]^+)$.

Synthesis of a Support, Hydrous Zirconia (ZrO_2). Hydrous zirconia (ZrO_2) was synthesized according to the procedure reported by Bhatt and Patel.[18]

Synthesis of a Catalyst, Supporting of VOL_2 onto ZrO_2. A series of catalysts containing VOL_2 (10–40%) were synthesized by impregnating ZrO_2 (1 g) with an aqueous solution of $VOL_2 \cdot H_2O$ (0.1–0.4 g/10–40 mL of conductivity water) and dried at 100 °C for 10 h. The obtained materials were designated as 10%, 20%, 30%, and 40% VOL_2/ZrO_2.

Single-Crystal X-ray Study. The crystal used for data collection was of dimensions 0.30 × 0.20 × 0.10 mm. The cell dimensions were determined by a least-squares fit of the angular settings of 5634 reflections in the θ range 3.32–29.07°. The intensities were measured by ϕ and ω scan modes for the θ range 3.34–24.00°. A total of 3037 reflections were treated as observed $[I > 2\sigma(I)]$. Data were corrected for Lorentz, polarization, and absorption factors. The structure was solved by direct methods using *SHELXS97*.[21] All non-H atoms of the molecule were located in the best E map. Full-matrix least-squares refinement was carried out using *SHELXL97*.[21]

All H atoms except water H atoms were included as idealized atoms riding on the respective C atoms with C−H bond lengths appropriate to the C-atom hybridization. Water H atoms were located from a difference Fourier map and included in the refinement. The final refinement cycles converged to $R = 0.0768$ and $R_w(F^2) = 0.1795$ for the observed data. Residual electron densities ranged from −0.370 to 0.374 e Å^{-3}. Atomic scattering factors were taken from *International Tables for X-ray Crystallography* (1992, Vol. C, Tables 4.2.6.8 and 6.1.1.4). CCDC 817984 contains the supplementary crystallographic data for this paper.

RESULTS AND DISCUSSION

The synthesized ligand was characterized by IR, ^{1}H and ^{13}C NMR, elemental analyses, and MS spectra. All spectral data agreed with the ligand structure. The oxovanadium(IV) complex having the general composition $VOL_2 \cdot H_2O$ has been synthesized by a general procedure based on the mixing of an aqueous solution of $VOSO_4 \cdot 5H_2O$ with an ethanol solution of the ligand in a 1:2 molar ratio and isolation of the final precipitate by filtration. The complex is stable to air and moisture, without any kind of decomposition also after several months. The complex is insoluble in water but soluble in chlorinated solvents, alcohols, acetonitrile, *N,N*-dimethylformamide (DMF), and dimethyl sulfoxide.

The crystallographic data are summarized in Table 1. An ORTEP view of the title compound with atomic labeling is shown in Figure 1.[22] As per our knowledge, there is only one crystal structure of the vanadium complex of the acylpyrazolone ligand that has been reported in the literature[16] having acylpyrazolonate ligands in the anti configuration to each other. Single-crystal data reveal that the two O,O-chelating acylpyrazolonate ligands occupy the equatorial plane of the oxovanadium(IV) complex in a syn configuration to each other, which is in contrast to the structure published elsewhere,[16] and the distorted octahedral geometry exists through coordination to the vanadium center of a water molecule trans to the oxo group. Thus, the ligand forms a six-membered chelate ring with the vanadium metal center. The V−O bond distances of the two chelated acylpyrazolonate ligands are in the range 1.96–2.02 Å. The average "bite" angles are 88.3(1) and 90.2(1)°.

Selected bond distances and bond angles are listed in Table 2. H atoms are shown as small spheres of arbitrary radii. The

Table 2. Selected Bond Lengths (Å) and Bond Angles (deg)^a

V1−O41	1.593(4)	V1−O3	1.969(3)
V1−O23	1.978(3)	V1−O13	1.999(3)
V1−O33	2.022(3)	V1−O42	2.247(4)
O41−V1−O3	99.10(18)	O41−V1−O23	100.31(16)
O3−V1−O23	87.49(13)	O41−V1−O13	96.91(16)
O3−V1−O13	88.31(13)	O23−V1−O13	162.72(14)
O41−V1−O33	95.60(18)	O3−V1−O33	165.30(15)
O23−V1−O33	90.24(13)	O13−V1−O33	89.58(13)
O41−V1−O42	175.42(19)	O3−V1−O42	84.13(15)
O23−V1−O42	83.03(15)	O13−V1−O42	79.87(14)
O33−V1−O42	81.18(15)		

^{a}Estimated standard deviations are given in parentheses.

geometry of the molecule was calculated using *WinGX*[23] and *PARST*[24] software. Examination of nonbonded contacts reveals O−H⋯N, C−H⋯O, and C−H⋯π intermolecular hydrogen bonds (Table 3), which are responsible for the stability of the molecules within the unit cell. The packing of molecules in the

Table 3. O−H⋯N, C−H⋯O, and C−H⋯π Hydrogen-Bonding Geometry^a

D−H⋯A^b	D−H (Å)	D⋯A (Å)	H⋯A (Å)	D−H⋯A (deg)
O42−H421⋯N1i	0.80(6)	2.851(5)	2.09(6)	159(6)
C30−H30⋯O41ii	0.93(1)	3.248(8)	2.425(4)	148(4)
O42−H422⋯N21iii	0.80(4)	2.904(6)	2.16(5)	156(4)
C35−H35⋯Cg4iii	0.93(1)	3.498(7)	2.639(4)	154(4)

^{a}Cg4 represents the center of gravity of the ring C26−C31. ^{b}Symmetry code: i, x, $-y + 1/2$, $+z + 1/2$; ii, $-x$, $-y$, $-z + 1$; iii, $-x$, $-y$, $-z + 2$.

unit cell is further stabilized by π−π-stacking interactions (Figure 2). A summary of π−π interactions is given in Table 4.

The vanadium and zirconium contents in 30% VOL_2/ZrO_2 were measured by ICP analysis. Found: Zr, 49.88; V, 1.72 (calcd: Zr, 49.69; V, 1.76).

TGA was performed for VOL_2 and 30% VOL_2/ZrO_2. TGA of VOL_2 shows a weight loss of 2.96% within the range of 50–150 °C, which corresponds to a loss of the coordinated water molecule. The decomposition of the VOL_2 complex was observed in several steps from 300 °C. The data indicate that the complex is stable to decomposition up to 300 °C.

TGA of 30% VOL_2/ZrO_2 shows an initial weight loss up to 150 °C, maybe due to the removal of adsorbed water molecules. No significant loss occurs up to 350 °C, which indicates an increase in the stability of VOL_2 after supporting ZrO_2.

DTA of VOL_2 shows endothermic peaks at 80 and 235 °C, due to the loss of adsorbed water and coordinating water, respectively. In addition, DTA of VOL_2 shows a decomposition temperature at 300 °C. DTA of 30% VOL_2/ZrO_2 shows a small endotherm due to the loss of adsorbed water. No significant loss up to 350 °C is observed, which indicates that the present material is stable up to 350 °C.

FT-IR was recorded to confirm the presence of reactive undegraded VOL_2 species present on the surface of ZrO_2. The
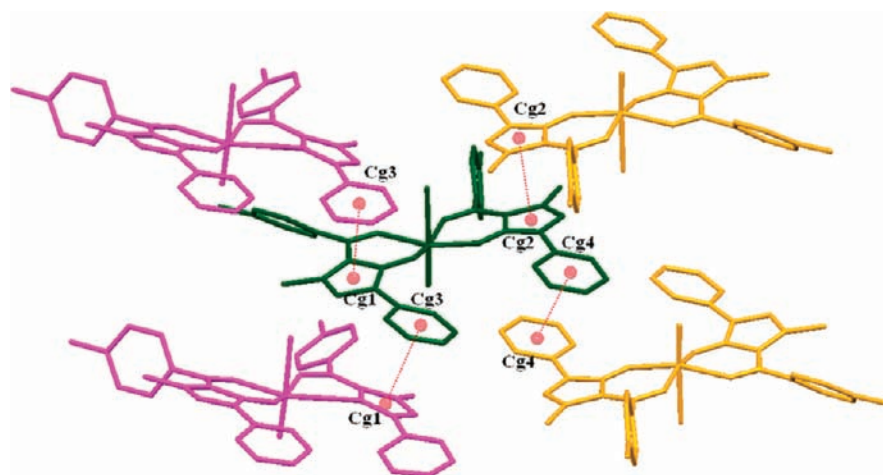
Figure 2. View of the layers formed by intermolecular π-stacking interactions of VOL$_2$. Different colors represent different chains formed by $\pi-\pi$ interaction. Cg1, Cg2, Cg3, and Cg4 represent ring N1, N2, and C3−C5, ring N21, N22, and C23−C25, ring C6−C11, and ring C26−C31, respectively. H atoms were omitted for clarity.

Table 4. Geometry of $\pi-\pi$ Interactions[a]

1CgI−CgJ[b]	CgI...CgJ(Å)	CgI...P(Å)	α (deg)	β (deg)	Δ (Å)
Cg1-Cg3i	3.677(4)	3.645	8.51	12.53	0.48
Cg2-Cg2ii	3.702(3)	3.665	0.00	8.14	0.52
Cg3-Cg1iii	3.677(4)	3.589	8.51	7.55	0.80
Cg4-Cg4iv	3.797(4)	3.631	0.00	17.02	1.11

[a]Cg represents the center of gravity of the following rings: Cg1 ring (N1, N2, C3−C5), Cg2 ring (N21, N22, C23−C25), Cg3 ring (C6−C11), and Cg4 ring (C26−C31). CgI···CgJ represents the distance between the ring centroids ; CgI···P is the perpendicular distance of the centroid of one ring from the plane of the other. α is the dihedral angle between the planes of rings I and J; β is the angle between normal to the centroid of ring I and the line joining ring centroids; Δ is the displacement of the centroid of ring J relative to the intersection point of the normal to the centroid of ring I and the least-squares plane of ring J. [b]Symmetry code: i, x, $^1/_2 - y$, $^1/_2 + z$; ii, $-x$, $-y$, $2 - z$; iii, x, $^1/_2 - y$, $-^1/_2 + z$; iv, $-x$, $-y$, $1 - z$.

FT-IR spectrum of VOL$_2$ exhibits a band at 3395 cm^{-1}, which can be assigned to the coordinated water. The complex shows absorptions at 1567 and 1476 cm^{-1}, which are due to $\nu_{C=N}$ of the pyrazolone ring and ν_{C-O}. The vanadium complex shows a strong band at 966 cm^{-1} due to $\nu_{V=O}$ stretching. The band at 476 cm^{-1} is assigned to ν_{V-O}. The FT-IR spectrum of 30% VOL$_2$/ZrO$_2$ shows that all of the bands correspond to functional groups of VOL$_2$, indicating the presence of VOL$_2$ over the surface of the catalyst. The shifting of the band values may be due to interaction of the oxygen of VOL$_2$ with the hydrogen of the surface hydroxyl groups of ZrO$_2$.

The full-range (3200−2000 G) X-band ESR spectra for VOL$_2$ (frozen solution state and room temperature solid state) and VOL$_2$/ZrO$_2$ (room temperature) were recorded (Figure 3). The ESR spectra of VOL$_2$ at liquid-nitrogen temperature and room temperature are shown in Figure 3a. X-band EPR spectra were recorded in DMF for VOL$_2$. The ESR spectrum of the metal complex provides information about hyperfine and superhyperfine structures, which is important in the study of the metal-ion environment in the complexes, i.e., the geometry, the nature of the ligating sites from the ligand of the metal, and the degree of covalency of the metal−ligand bonds.

The room temperature (300 K) spectrum of VOL$_2$ (Figure 3b) is a typical 8-line pattern, which shows that a single
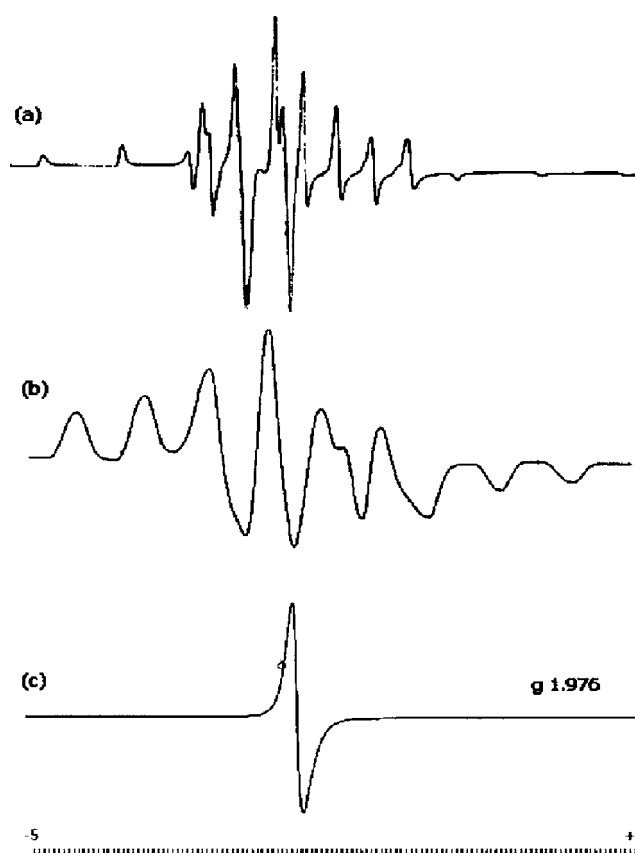
Figure 3. ESR spectra of (a) VOL$_2$ (in DMF at liquid-nitrogen temperature), (b) VOL$_2$ (in a polycrystalline state at room temperature), and (c) VOL$_2$/ZrO$_2$ (in a polycrystalline state at room temperature).

vanadium is present in the molecule; i.e., it is mononuclear. In the frozen solution state, the spectrum shows two types of resonance components, one set due to the parallel feature and the other set due to the perpendicular feature, which indicates axially symmetric anisotropy with a well-resolved 16-line hyperfine splitting, characteristic of interaction between the electron and vanadium nuclear spins. The g values were

computed from the spectra using a tetracyanoethylene free radical as the g marker.

The room temperature ESR of VOL_2/ZrO_2 (Figure 3c) shows single-line spectra (V^{4+} $3d^1$) with a g value of 1.976, confirming the presence of vanadium(IV) in octahedral symmetry on the surface of the support. The absence of hyperfine lines may be due to support of VOL_2 onto ZrO_2.

The larger surface area of 30% VOL_2/ZrO_2 (85.97 m^2 g^{-1}) compared to that of VOL_2 (2.13 m^2 g^{-1}) was due to support of VOL_2, and it is as expected.

The nitrogen adsorption isotherm of 30% VOL_2/ZrO_2 (Figure 4a) presents a type II isotherm with a hysteresis loop in the desorption isotherm in the high range of relative
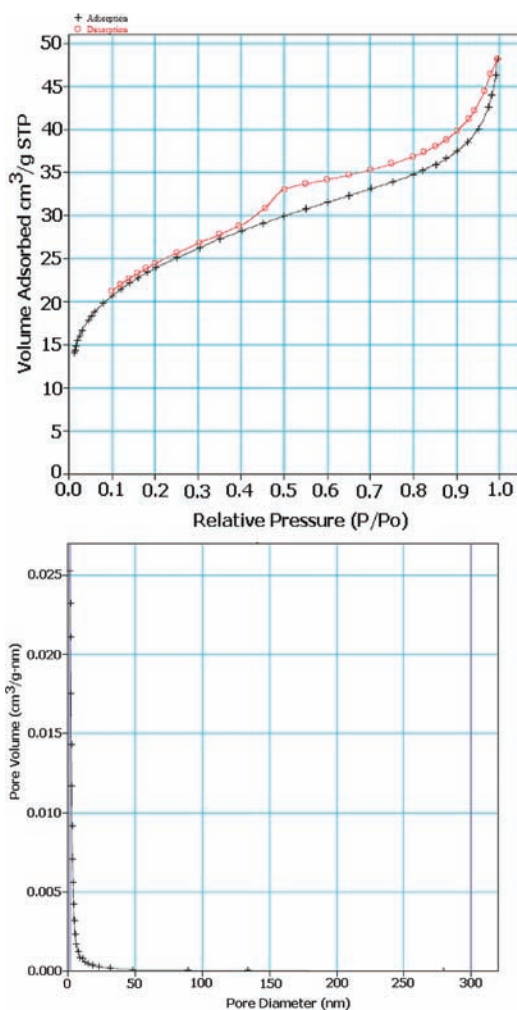

Figure 4. BET isotherm of 30% VOL_2/ZrO_2: (a) adsorption–desorption isotherm; (b) pore-size distribution.

pressure. The type II isotherm is obtained when adsorption occurs on nonporous powders or on powders with pore diameters larger than the micropores. The inflection point or knee of the isotherm usually occurs near completion of the first adsorbed monolayer and, with increasing relative pressure, second and higher layers are completed until at saturation the number of adsorbed layers becomes infinite.

The pore-size distribution curve for 30% VOL_2/ZrO_2 shows a maximum at 10−15 nm (Figure 4b), which indicates pores with sizes belonging to the entire range of the characteristic

mesoporosity. The sharp pore-size distribution in the maximum range shows the uniformity of the porous structure.

The SEM images of ZrO_2, VOL_2, and 30% VOL_2/ZrO_2 at a magnification of 100× are reported in Figure 5. Figure 5b
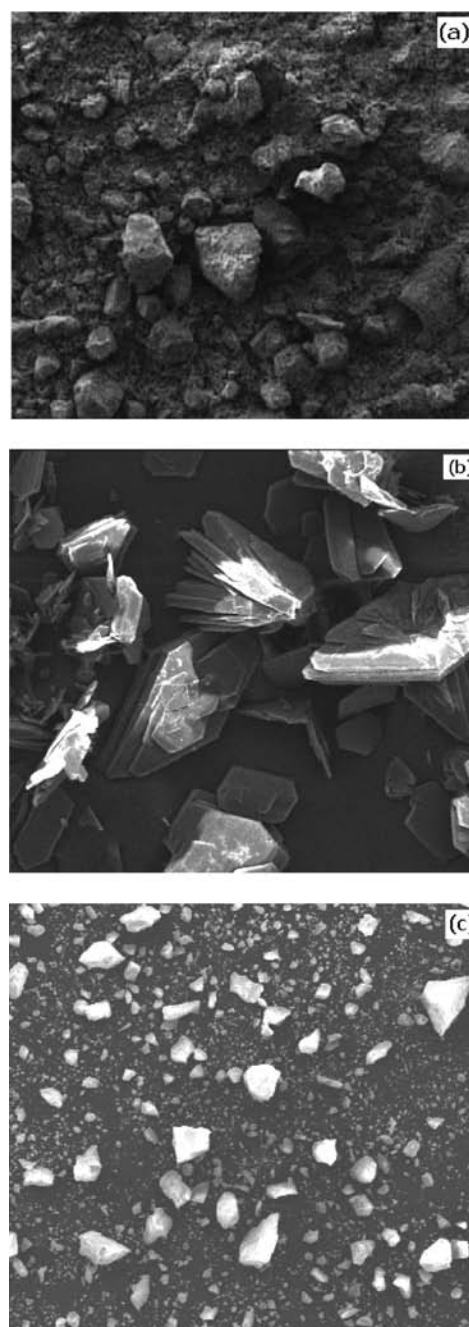
Figure 5. SEM images of (a) ZrO_2, (b) VOL_2, and (c) 30% VOL_2/ZrO_2 at a magnification 100×.

shows the crystalline nature of VOL_2 (block-shaped). It is seen from the SEM image of 30% VOL_2/ZrO_2 (Figure 5c) that the surface of the support is distinctly altered after support of VOL_2 onto ZrO_2. The SEM image of 30% VOL_2/ZrO_2 shows a uniform dispersion of particles. SEM confirms the uniform as well as high dispersion of VOL_2 in a noncrystalline form onto the surface of the support.

Oxidation of Styrene Using H_2O_2. The reaction was carried out by varying the mole ratio of styrene to H_2O_2 with

25 mg of the catalyst for 24 h at 80 °C. Generally, styrene oxidation gives styrene oxide, benzaldehyde, benzyl alcohol, acetophenone, and benzoic acid. However, in the present reaction conditions, the major oxidation product obtained was benzaldehyde maybe because of (i) the direct oxidative cleavage of C=C of styrene and (ii) the fast conversion of styrene oxide to benzaldehyde.

With a 1:3 molar ratio, the conversion of styrene was >99% and the selectivity for benzaldehyde was 99.1%, while with a 1:4 molar ratio, the conversion was >99% with 78% selectivity for benzaldehyde. Hence, further optimization of the conditions was carried out with a 1:3 molar ratio.

Effect of the Percent Loading of VOL_2. The oxidations of styrene carried out with H_2O_2 in 1:3 molar ratios by using 25 mg of fresh catalysts for 24 h at 80 °C are presented in Figure 6. The figure shows an increase in the conversion with an increase in the percent loading of VOL_2 from 10% to 30%.
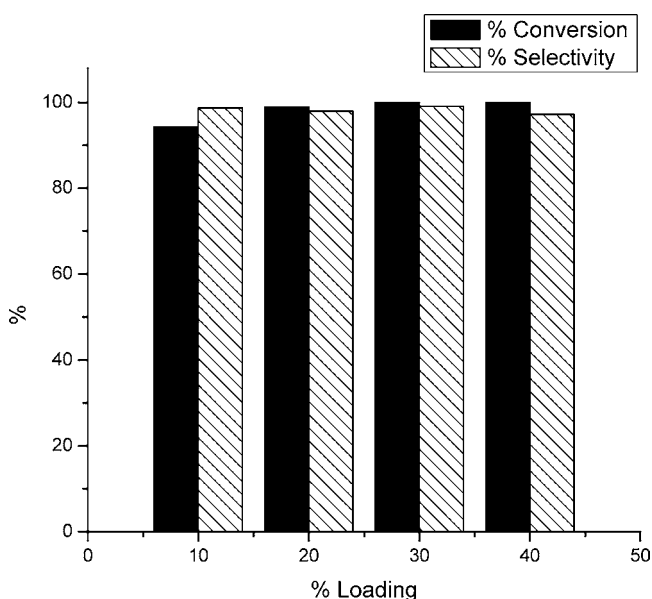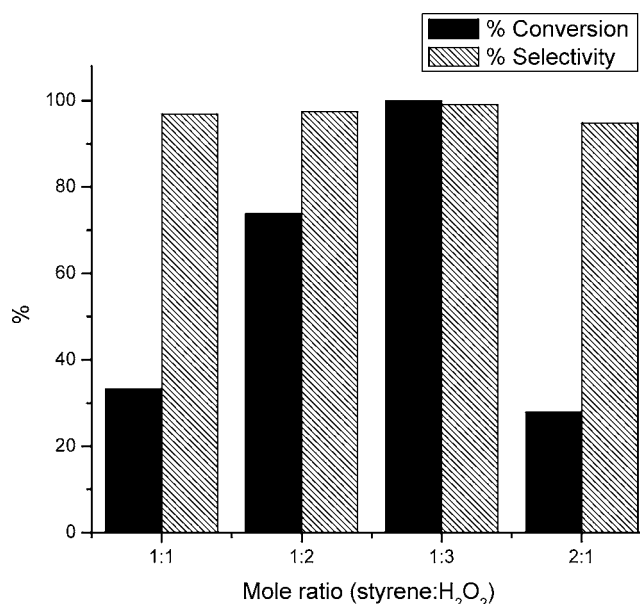

Figure 6. Effect of the percent loading. Percent conversion is based on styrene; time = 24 h; temperature = 80 °C; amount of catalyst = 25 mg, molar ratio of styrene to H_2O_2 = 1:3.

Further, with an increase in the percent loading from 30% to 40%, a small decrease in conversion was found. This may be due to blocking of the active sites. Thus, the loading of VOL_2 on the support was fixed at 30%. A detailed study was carried out at 80 °C over 30% VOL_2/ZrO_2.
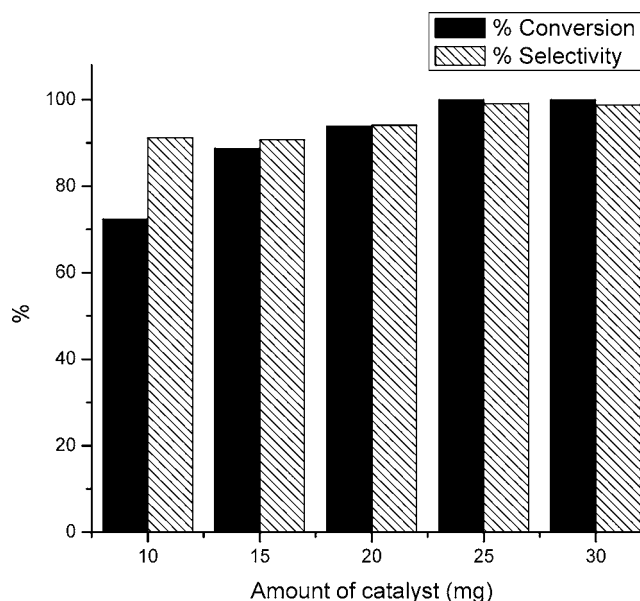
Effect of the Mole Ratio of Styrene to H_2O_2. In order to determine the effect of H_2O_2 on the oxidation of styrene to benzaldehyde, the mole ratio of styrene to H_2O_2 was varied (1:1, 1:2, 1:3, and 2:1), keeping other parameters fixed: namely, catalyst (25 mg), temperature (80 °C), and reaction time (24 h). The results are shown in Figure 7. Styrene to H_2O_2 molar ratios of 1:1 and 1:2 resulted in 33.2 and 73.8% conversion, respectively, and when the styrene to H_2O_2 molar ratio was changed to 1:3, conversion increased to 100%, keeping all other conditions similar.

However, conversion was found to decrease for a styrene to H_2O_2 molar ratio of 2:1. Therefore, a 1:3 molar ratio of styrene to H_2O_2 was found to be the optimum in terms of conversion of styrene.

Figure 7. Effect of the mole ratio. Percent conversion is based on styrene; time = 24 h; temperature = 80 °C; amount of catalyst = 25 mg.

Effect of the Amount of Catalyst. The amount of catalyst has a significant effect on the oxidation of styrene. Five different amounts of 30% VOL_2/ZrO_2, viz., 10, 15, 20, 25, and 30 mg, were used, keeping all other reaction parameters fixed: namely, temperature (80 °C), styrene (10 mmol), 30% H_2O_2 (30 mmol), and reaction time (24 h). The results are shown in Figure 8, indicating 72.4, 88.7, 93.9, 100, and 100% conversion

Figure 8. Effect of the amount of catalyst. Percent conversion is based on styrene; time = 24 h; temperature = 80 °C; molar ratio of styrene to H_2O_2 = 1:3.

corresponding to 10, 15, 20, 25, and 30 mg of catalyst, respectively.

The lower conversion of styrene into benzaldehyde with 10–20 mg of catalyst may be due to fewer catalytic sites. The maximum percentage conversion was observed with 25 mg of

catalyst, but there was no remarkable difference in the progress of the reaction when 25 or 30 mg of catalyst was employed. Therefore, 25 mg of catalyst was taken to be optimal.

Effect of the Reaction Time. The time dependence of the catalytic solvent-free oxidation of styrene was studied by performing the reaction of styrene (10 mmol) with 30% H_2O_2 (30 mmol) in the presence of 25 mg of catalyst at 80 °C with constant stirring. The percent conversion was monitored at different reaction times.

It is seen from Figure 9 that, with an increase in the reaction time, percent conversion also increases. The initial conversion
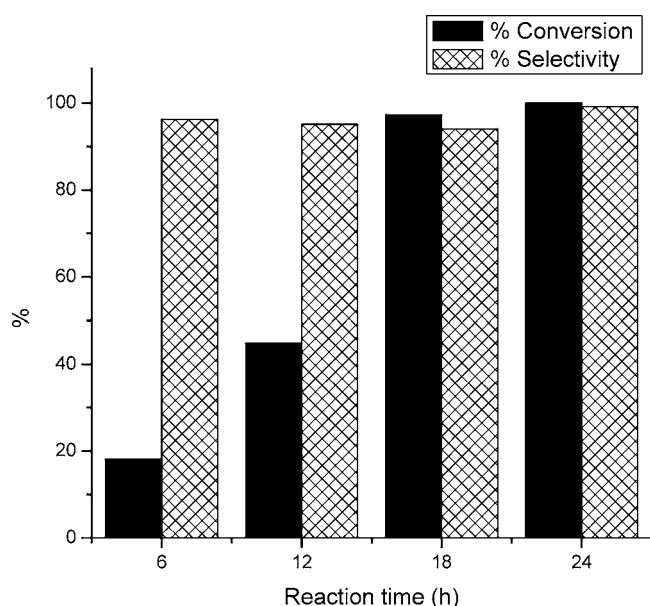
Figure 9. Effect of the reaction time. Percent conversion is based on styrene; amount of catalyst = 25 mg; temperature = 80 °C; molar ratio of styrene to H_2O_2 = 1:3.

of styrene increased with the reaction time. This is because more time is required for the formation of a reactive intermediate (substrate + catalyst), which is finally converted into the products. It is seen that maximum conversion of styrene was observed within 24 h.

The optimum conditions for maximum percent conversion of styrene to benzaldehyde are a mole ratio of styrene to H_2O_2 of 1:3, with 25 mg of catalyst and 24 h reaction time at 80 °C.

The control experiments with ZrO_2 and VOL_2 were also carried out under optimized conditions with styrene and H_2O_2 as well as benzyl alcohol and H_2O_2.

It can be seen from Table 5 that ZrO_2 is inactive toward the oxidation of styrene, indicating that the catalytic activity is due

Table 5. Control Experiments for the Oxidation of Styrene[a]

catalyst	% conversion	% selectivity of benzaldehyde
ZrO_2		
VOL_2	97.1	96.4

[a]Percent conversion is based on styrene; amount of VOL_2 = 5.8 mg, amount of ZrO_2 = 19.2 mg; styrene:H_2O_2 = 1:3; time = 24 h; temperature = 80 °C.

to only VOL_2. The same reaction was carried out by taking the active amount of VOL_2 (5.8 mg). It was found that the active catalyst gives 97% conversion of styrene with >96% selectivity

of benzaldehyde. Almost the same obtained activity for the supported catalyst indicates that VOL_2 is the real active species. Thus, we are successful in supporting VOL_2 onto ZrO_2 without any significant loss in activity and, hence, in overcoming the traditional problems of homogeneous catalysis.

Heterogeneity Test. A heterogeneity test was carried out for the oxidation of styrene. For the rigorous proof of heterogeneity, a test[25] was carried out by filtering the catalyst from the reaction mixture at 80 °C after 2 h, and then the filtrate was allowed to react up to 4 h. The 2 h reaction mixture and the filtrate were analyzed by gas chromatography. No change in percent conversion as well as percent selectivity was found, indicating that the present catalyst falls into category C.[26] The results are presented in Table 6.

Table 6. Heterogeneity Test[a]

catalyst	% conversion	% selectivity benzaldehyde
30% VOL_2/ZrO_2 (2 h)	15.4	90.3
filtrate (4 h)	15.6	89.7

[a]Percent conversion is based on styrene; amount of catalyst = 25 mg; molar ratio of styrene to H_2O_2 = 1:3, temperature = 80 °C.

Recycling of the Catalyst. The oxidation of styrene was carried out with the recycled catalyst, under optimized conditions.

The catalyst was removed from the reaction mixture after completion of the reaction by simple filtration, washed with dichloromethane, and dried at 100 °C. The catalyst was recycled in order to test its activity as well as stability. The obtained results are presented in Table 7. As can be seen from

Table 7. Oxidation of Styrene with Fresh and Recycled Catalysts[a]

| catalyst	cycle	% conversion	% selectivity benzaldehyde	TON
30% VOL_2/ZrO_2	fresh	100	99.1	1151
	1	99.8	98.9	1148
	2	99.2	97.0	1116

[a]Percent conversion is based on styrene; amount of catalyst = 25 mg; molar ratio of styrene to H_2O_2 = 1:3, time = 24 h; temperature = 80 °C.

table, there was no appreciable change observed in selectivity; however, a small decrease in conversion was observed, which shows that the catalysts are stable and can be regenerated for repeated use.

Reaction Mechanism. A reaction mechanism for the oxidation of styrene is proposed in Scheme 3. For the catalytic reaction to proceed, the activation of V^{4+} is required. The activation of V^{4+} species takes place through the attack of H_2O_2 followed by the formation of intermediate $HOOV^{5+}(OH)L_2/ZrO_2$. Upon rearrangement of this intermediate, an active species $^\bullet OOV^{5+}OL_2/ZrO_2$ is formed. This formed active species is responsible for the activation of alkenes.

This activated species $^\bullet OOV^{5+}OL_2/ZrO_2$ radical (i.e., V–O_2 metal–superoxo intermediate), which then attacks the substrate reversibly, binds to the alkene attacking the reaction site, resulting in the oxidation of substrate to form products. Further, the oxidation of alkenes via a radical-chain mechanism is a known process.[27,28] In order to confirm the role of the formed active intermediate $^\bullet OOV^{5+}OL_2/ZrO_2$, it was isolated

Scheme 3. Proposed Reaction Mechanism for the Oxidation of Styrene
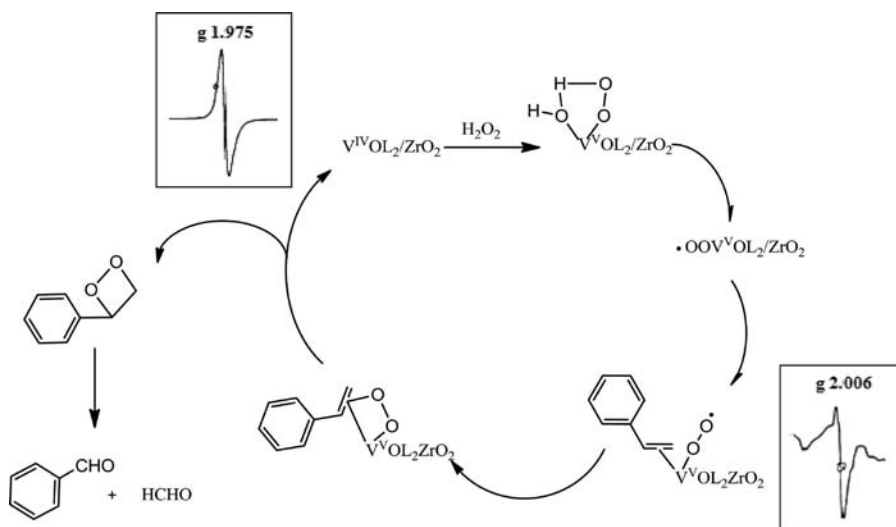
and characterized by ESR. The room temperature X-band ESR of $V^{4+}OL_2/ZrO_2$ shows an ESR signal with a g value of 1.975, which may correspond to V^{4+} in octahedral symmetry. The room temperature X-band ESR of the active intermediate ($^{\bullet}OOV^{5+}OL_2/ZrO_2$) shows a typical anisotropic ESR with splitting of the ESR signal, which may be due to the presence of a radical electron.

The broadening of the signal may be due to the presence of a transition-metal ion. The anisotropic ESR signal is indicative of the presence of a free radical. The free radical resides on an O atom, and it is strongly coupled with V^{5+}. The average g value calculated for the present system ($^{\bullet}OOV^{5+}OL_2/ZrO_2$) is 2.006, which are in good agreement with the reported g value of organic free radicals, 2.0023.[29] The ESR studies strongly support the proposed mechanism.

CONCLUSION

An oxovanadium(IV) complex containing a 1-phenyl-3-methyl-4-toluoyl-5-pyrazolone donor ligand has been synthesized, and its crystal and molecular structures have been resolved by single-crystal XRD, showing a distorted octahedral environment around vanadium through coordination of two O,O-chelating acylpyrazolonate ligands occupying the equatorial plane in a syn configuration to each other and a water molecule trans to the oxo group. The catalyst comprising the oxovanadium(IV) complex and hydrous zirconia has proven to be successful in the oxidation of styrene under mild reaction conditions. The superiority of the catalyst lies in obtaining 100% conversion of styrene with >99% selectivity for benzaldehyde (1151 TON). In all reactions, removal of the catalyst consists of single filtration, and the catalyst can be reused after a simple workup.

ASSOCIATED CONTENT

Ⓢ Supporting Information

Further details (Figures S1−S7). This material is available free of charge via the Internet at http://pubs.acs.org.

AUTHOR INFORMATION

Corresponding Author

*E-mail: rajendra_jadeja@yahoo.com (R.N.J.), aupatel_chem@yahoo.com. (A.P.). Tel: +91 265 2795552 (R.N.J.), +91 265 6595697 (A.P.).

REFERENCES

(1) (a) Rehder, D. *Coord. Chem. Rev.* **1999**, *182*, 297−322. (b) Frafflsto da Silva, J. J. R.; Williams, R. J. P. *The Biological Chemistry of the Elements, The Inorganic Chemistry of Life*, 2nd ed.; Oxford University Press: Oxford, U.K., 2001. (c) Kaim, W.; Schwederski, B. *Bioinorganic Chemistry: Inorganic Elements in the Chemistry of Life*; John Wiley & Sons: Chichester, U.K., 1994. (d) Eady, R. R. *Coord. Chem. Rev.* **2003**, *237*, 23−30.

(2) (a) Rehder, D. *J. Inorg. Biochem.* **2008**, *102*, 1152−1158. (b) Maurya, M. R.; Agarwal, S.; Bader, C.; Rehder, D. *Eur. J. Inorg. Chem.* **2005**, *147*−157. (c) Rehder, D.; Santonin, G.; Licini, G. M.; Schulzke, C.; Meier, B. *Coord. Chem. Rev.* **2003**, *237*, 53−63. (d) Plass, W. *Coord. Chem. Rev.* **2003**, *237*, 205−212. (e) Thompson, K. H.; Orvig, C. *Coord. Chem. Rev.* **2001**, *219*, 1033−1053. (f) Butler, A. *Coord. Chem. Rev.* **1999**, *187*, 17−35.

(3) (a) Osinska-Krolicka, I.; Podsiadly, H.; Bukietynska, A. *J. Inorg. Biochem.* **2004**, *98*, 2087−2098. (b) Thompson, K. H.; McNeil, J. H.; Orvig, C. *Chem. Rev.* **1999**, *99*, 2561−2572.

(4) (a) Crans, D. C. *Pure Appl. Chem.* **2005**, *77*, 1497−1527. (b) Sakurai, H.; Kojima, Y.; Yoshikawa, Y.; Kawabe, K.; Yasuri, H. *Coord. Chem. Rev.* **2002**, *226*, 187−198. (c) Shechter, Y.; Goldwaser, I.; Mironchik, M.; Fridkin, M.; Gefel, D. *Coord. Chem. Rev.* **2003**, *237*, 3−11.

(5) (a) Shechter, Y.; Karlish, S. J. D. *Nature* **1980**, *286*, 556−558. (b) Shechter, Y. *Diabetes* **1990**, *39*, 1−5.

(6) (a) Rehder, D. *Bioinorganic Vanadium Chemistry*; John Wiley & Sons: Chichester, U.K., 2008. (b) Kustin, K., Pessoa, J. C., Crans, D. C., Eds. *Vanadium: The Versatile Metal*; American Chemical Society: Washington, DC, 2007. (c) Richards, R. L. In *Encyclopedia of Inorganic*

Chemistry, 2nd ed.; King, R. B., Ed.; Wiley: New York, 2005; Vol. *IX*, pp 5767–5803. (d) Hirao, T. *Chem. Rev.* **1997**, *97*, 2707–2724. (e) Tracey, A. S.; Willsky, G. R.; Takeuchi, E. S. *Vanadium Chemistry, Biochemistry Pharmacology and Practical Applications*; CRC Press: Boca Raton, FL, 2007.

(7) (a) Kuznetsov, M. L.; Pessoa, J. C. *Dalton Trans.* **2009**, 5460–5468. (b) Mizuno, H.; Sakurai, H.; Amaya, T.; Hirao, T. *Chem. Commun.* **2006**, 5042–5044. (c) Cuervo, L. G.; Kozlov, Y. N.; Süss-Fink, G.; Shul'pin, G. B. *J. Mol. Catal. A: Chem.* **2004**, *218*, 171–177.

(8) (a) Bolm, C. *Coord. Chem. Rev.* **2003**, *237*, 245–256. (b) Du, G.; Espenson, J. H. *Inorg. Chem.* **2005**, *44*, 2465–2471.

(9) Belokon, Y. N.; North, M.; Maleev, V. I.; Voskoboev, N. V.; Moskalenko, M. A.; Preegudov, A. S.; Dmitriev, A. V.; Ikonnikov, N. S.; Kagan, H. B. *Angew. Chem., Int. Ed.* **2004**, *43*, 4085–4089.

(10) (a) Michaelson, R. C.; Palermo, R. E.; Sharpless, K. B. *J. Am. Chem. Soc.* **1977**, *99*, 1990–1992. (b) Hoshino, Y.; Yamamoto, H. *J. Am. Chem. Soc.* **2000**, *122*, 10452–10453. (c) Bolm, C.; Kühn, T. *Synlett* **2000**, *6*, 899–901. (d) Wu, H. L.; Uang, B. J. *Tetrahedron: Asymmetry* **2002**, *13*, 2625–2628. (e) Adam, W.; Beck, A. K.; Pichota, A.; Saha-Möller, C. R.; Seebach, D.; Vogl, N.; Zhang, R. *Tetrahedron: Asymmetry* **2003**, *14*, 1355–1361. (f) Zhang, W.; Basak, A.; Kosugi, Y.; Hoshino, Y.; Yamamoto, H. *Angew. Chem., Int. Ed.* **2005**, *44*, 4389–4391. (g) Bourhani, Z.; Malkov, A. V. *Chem. Commun.* **2005**, 4592–4594. (h) Lattanzi, A.; Piccirillo, S.; Scettri, A. *Eur. J. Org. Chem.* **2005**, 1669–1674.

(11) (a) Chu, C. Y.; Hwang, D. R.; Wang, S. K.; Uang, B. J. *Chem. Commun.* **2001**, 980–981. (b) Luo, Z.; Liu, Q.; Gong, L.; Cui, X.; Mi, A.; Jiang, Y. *Angew. Chem., Int. Ed.* **2002**, *41*, 4532–4535. (c) Barhate, N. B.; Chen, C. T. *Org. Lett.* **2002**, *4*, 2529–2532. (d) Somei, H.; Asano, Y.; Yoshida, T.; Takizawa, S.; Yamataka, H.; Sasai, H. *Tetrahedron Lett.* **2004**, *45*, 1841–1844.

(12) (a) Nakajima, K.; Kojima, M.; Fujita, J. *Chem. Lett.* **1986**, 1483–1486. (b) Cogoa, D. A.; Liu, G.; Kim, K.; Backes, B. J.; Ellman, J. A. *J. Am. Chem. Soc.* **1998**, *120*, 8011–8019. (c) Pelotier, B.; Anson, M. S.; Campbell, I. B.; Macdonald, S. J. F.; Priem, G.; Jackson, R. F. W. *Synlett* **2002**, 1055–1060. (d) Ohta, C.; Shimizu, H.; Kondo, A.; Katsuki, T. *Synlett* **2002**, 161–163. (e) Santoni, G.; Licini, G.; Rehder, D. *Chem.—Eur. J.* **2003**, *9*, 4700–4708. (f) Sun, J.; Zhu, C.; Dai, Z.; Yang, M.; Pan, Y.; Hu, H. *J. Org. Chem.* **2004**, *69*, 8500–8503. (g) Drago, C.; Caggiano, L.; Jackson, R. F. W. *Angew. Chem., Int. Ed.* **2005**, *44*, 7221–7223. (h) Basak, A.; Barlan, A. U.; Yamamoto, H. *Tetrahedron: Asymmetry* **2006**, *17*, 508–511.

(13) Hsieh, S. H.; Gau, H. M. *Synlett* **2006**, 1871–1874.

(14) (a) Akai, S.; Tanimoto, K.; Kanao, Y.; Egi, M.; Yamamoto, T.; Kita, Y. *J. Am. Chem. Soc.* **2005**, *127*, 1090–1091. (b) Blanc, A.; Toste, F. D. *Angew. Chem., Int. Ed.* **2006**, *45*, 2096–2099.

(15) (a) Pomogăilo, A. D. *Catalysis by Polymer-Immobilized Metal Complexes*; CRC Press: New York, 1998. (b) Leadbeater, N. E.; Marco, M. *Chem. Rev.* **2002**, *102*, 3217–3274. (c) Burgess, K. *Solid Phase Organic Synthesis*; John Wiley: New York, 2000.

(16) Marchetti, F.; Pettinari, C.; Nicola, C. D.; Pettinari, R.; Crispini, A.; Crucianelli, M.; Giuseppe, A. D. *Appl. Catal. A* **2010**, *378*, 211–233.

(17) Maurya, M. R.; Bisht, M.; Kumar, A.; Kuznetsov, M. L.; Avecilla, F.; Pessoa, J. C. *Dalton Trans.* **2011**, *40*, 6968–6983.

(18) Bhatt, N.; Patel, A. *J. Mol. Catal. A: Chem.* **2005**, *238*, 223–228.

(19) Pathan, S.; Patel, A. *Dalton Trans.* **2011**, *40*, 348–355 and references cited therein.

(20) (a) Jadeja, R. N.; Shah, J. R.; Suresh, E.; Paul, P. *Polyhedron* **2004**, *23*, 2465–2474. (b) Jadeja, R. N.; Shah, J. R. *Polyhedron* **2007**, *26*, 1677–1681. (c) Jadeja, R. N.; Vyas K. M.; Gupta V. K.; Joshi R. G.; Prabha C. R *Polyhedron* **2011**, DOI:10.1016/j.poly.2011.11.004.

(21) Sheldrick, G. M. *SHELX97*; University of Göttingen: Göttingen, Germany, 1997.

(22) Farrugia, L. J. *J. Appl. Crystallogr.* **1997**, *30*, 565–566.

(23) Farrugia, L. J. *J. Appl. Crystallogr.* **1999**, *32*, 837–838.

(24) Nardelli, M. *J. Appl. Crystallogr.* **1995**, *28*, 659.

(25) Okuhara, T.; Mizuno, N.; Misono, M. *Adv. Catal.* **1996**, *41*, 130.

(26) Sheldon, A.; Walau, M.; Arends, I. W. C. E.; Schuchurdt, U. *Acc. Chem. Res.* **1998**, *31*, 485–493.

(27) Xinrong, L.; Jinyu, X.; Huizhang, L.; Bin, Y.; Songlin, J.; Gaoyang, X. *J. Mol. Catal. A: Chem.* **2000**, *161*, 163–169.

(28) Zhang, X.; Chen, Q.; Duncan, D. C.; Lachicotte, R. J.; Hill, C. L. *Inorg. Chem.* **1997**, *36*, 4381–4386.

(29) Bersohn, M.; Baird, J. C. *An Introduction to Electron Paramagnetic Resonance*; W. A. Benjamin, Inc.: New York, 1966; Chapter 5, p 69.

■ NOTE ADDED AFTER ASAP PUBLICATION

This paper was published on the Web on December 21, 2011, with an error in Scheme 3. The corrected version was reposted on December 28, 2011. Additional text corrections were made and the paper was reposted on January 4, 2012.